

Journal Pre-proof

Mechanism of the Effects of Sodium Channel Blockade on the Arrhythmogenic Substrate of Brugada Syndrome

Koonlawee Nademanee, MD, Gumpanart Veerakul, MD, Akihiko Nogami, MD, Qing Lou, PhD, Méléze Hocini, MD, Ruben Coronel, MD, PhD, Elijah R. Behr, MD, Arthur Wilde, MD, PhD, Bastiaan J. Boukens, PhD, Michel Haissaguerre, MD

PII: S1547-5271(21)02323-7

DOI: <https://doi.org/10.1016/j.hrthm.2021.10.031>

Reference: HRTM 9028

To appear in: *Heart Rhythm*

Received Date: 25 October 2021

Accepted Date: 26 October 2021

Please cite this article as: Nademanee K, Veerakul G, Nogami A, Lou Q, Hocini M, Coronel R, Behr ER, Wilde A, Boukens BJ, Haissaguerre M, Mechanism of the Effects of Sodium Channel Blockade on the Arrhythmogenic Substrate of Brugada Syndrome, *Heart Rhythm* (2021), doi: <https://doi.org/10.1016/j.hrthm.2021.10.031>.

This is a PDF file of an article that has undergone enhancements after acceptance, such as the addition of a cover page and metadata, and formatting for readability, but it is not yet the definitive version of record. This version will undergo additional copyediting, typesetting and review before it is published in its final form, but we are providing this version to give early visibility of the article. Please note that, during the production process, errors may be discovered which could affect the content, and all legal disclaimers that apply to the journal pertain.

© 2021 Published by Elsevier Inc. on behalf of Heart Rhythm Society.



Mechanism of the Effects of Sodium Channel Blockade on the Arrhythmogenic Substrate of Brugada Syndrome

Koonlawee Nademanee, MD, Gumpanart Veerakul, MD, Akihiko Nogami, MD, Qing Lou, PhD, Méléze Hocini, MD, Ruben Coronel, MD, PhD, Elijah R Behr, MD, Arthur Wilde, MD, PhD, Bastiaan J. Boukens, PhD, Michel Haissaguerre, MD.

From Center of Excellence in Arrhythmia Research Chulalongkorn University, Bangkok Thailand (KN), Pacific Rim Electrophysiology Research Institute and Bumrungrad Hospital, Bangkok and Las Vegas (KN), Bhumipol Adulyadej RTAF Hospital (GV), CardioInsight Technologies, Medtronic, Minneapolis (QL), IHU Liryc, Electrophysiology and Heart Modeling Institute, Foundation Bordeaux Université, Pessac-Bordeaux (MH, MH, RC), University of Tsukuba, Japan (AN), Cardiology Clinical Academic Group, Institute of Molecular and Clinical Sciences, St. George's, University of London, and St. George's University Hospitals NHS Foundation Trust London, UK (EB), Heart Centre, Dept. of Clinical and Experimental Cardiology, Amsterdam University Medical Centres, location Academic Medical Center, Amsterdam, The Netherlands (RC, AW, BB).

Drs. Nademanee and Haissaguerre have research grants from Biosense Webster and Medtronic Inc. Lou Qing is an employee of CardioInsight Medtronic Inc. All

other authors have reported that they have no relationships relevant to the contents of this paper to disclose.

Correspondence: Koonlawee Nademanee, MD

Center of Excellence in Arrhythmia Research Chulalongkorn University.

Department of Medicine, Faculty of Medicine, Chulalongkorn University and Pacific Rim Electrophysiology Research Institute at Bumrungrad Hospital, Bangkok, Thailand.

Address: 1873 Rama IV Rd. Pathumwan, Bangkok 10330 Thailand

E-mail: wee@pacificcrimep.com

This work is partially supported by The National Research Council of Thailand & Grant in Aid from Bumrungrad Hospital, Bangkok, Thailand and Medtronic Inc. (KN). and by the Leducq Foundation (RHYTHM, 16CVD02, MH, MH, RC) and Predict 2 (AW). BJB was supported by the Dutch Heart Foundation (2016T047).

Total Word Count: 5000

Abstract

Background: The mechanisms by which sodium channel blockade and high-rate pacing modify electrogram substrates of Brugada syndrome (BrS) have not been elucidated.

Objectives: To determine the effect of ajmaline and high pacing rate on the BrS substrates.

Methods: Thirty-two BrS patients (age 40 ± 12 years) with frequent ventricular fibrillation (VF) episodes underwent right ventricular outflow tract (RVOT) substrate electroanatomical and electrocardiogram imaging (ECGI) mapping before and after ajmaline administration and during high-rate atrial pacing. In 4 patients, epicardial mapping was performed using open thoracotomy with targeted biopsies.

Results: Ajmaline increased the activation time delay in the substrate (33%; $p = 0.002$), ST elevation in the right precordial leads (74%; $p < 0.0001$), and the area of delayed activation (170%; $p < 0.0001$), coinciding with increased substrate size (75%; $p < 0.0001$). High atrial pacing rate increased the abnormal electrogram (EGM) duration at the RVOT areas from 112 ± 48 to 143 ± 66 ms ($p = 0.003$) and produced intermittent conduction block and/or excitation failure at the substrate sites, especially after ajmaline. Biopsies from the 4 patients with thoracotomy showed epicardial fibrosis where EGMs were normal at baseline but became fractionated after ajmaline. In some areas, local activation was absent and unipolar EGMs had a monophasic morphology resembling the shape of the action potential.

Conclusions: I_{Na} reduction with ajmaline severely compromises impulse conduction at the BrS fibrotic substrates by producing fractionated EGMs, conduction block, or excitation failure, leading to the Brugada ECG pattern and favoring VF genesis.

Key Words: Brugada Syndrome, catheter ablation, ion channelopathy, sudden death, sodium channel blocker.

Journal Pre-proof

Introduction

Sodium channel blockers (e.g., ajmaline, procainamide, flecainide) can unmask the typical coved type of ST elevation (STE) in the right precordial leads of BrS patients¹. However, how these drugs unmask the Brugada pattern and adversely affect the BrS substrate has not been clearly elucidated. An in-silico model has demonstrated that sodium current (I_{Na}) reduction creates activation block at sites of the current to load mismatch, leading to distal activation failure, local monophasic electrograms (EGM), and the typical ST-segment changes². This study aims to determine the effect of I_{Na} reduction by ajmaline and/or fast pacing rate on the RVOT epicardial substrates of symptomatic BrS patients.

Methods

Study Patients

BrS patients who had recurrent implantable cardioverter-defibrillator (ICD) discharges from VF episodes were enrolled into the study. All patients provided written informed consent, which had been approved by the Internal Ethics Review Board.

Study Protocol

The patients first underwent electroanatomical mapping of the BrS epicardial substrates using a ThermoCool catheter (Biosense Webster, Inc., Diamond Bar, CA) mapping/ablation catheters during sinus rhythm before and after ajmaline administration followed by electrophysiology studies including programmed stimulation for VF induction, as previously described³. A subset

of the study patients also underwent atrial pacing, either from the coronary sinus or high right atrium, with a decremental interval of 750, 600, 500, and 450 or 400 ms for 30 seconds or until Wenckebach periodicity or second-degree atrioventricular (AV) block occurred. During pacing, the mapping catheter was positioned at the RVOT substrate sites where fractionated EGM durations and late potentials were measured at baseline, pacing, and after ajmaline.

When non-invasive ECG imaging (ECGI; CardioInsight System, Medtronic, Inc., Minneapolis, MN) became available in our institutions, we added ECGI mapping for the arrhythmogenic substrates in our study protocol during baseline and after ajmaline infusion.

Mapping

Detailed epicardial and endocardial mapping of arrhythmogenic substrate of the RV as well as epicardial mapping of the left ventricle was performed during sinus rhythm. First, epicardial and endocardial electroanatomical mapping was performed using the voltage map software on the CARTO Navigation System (Biosense Webster, Inc.). An abnormal BrS substrate area was characterized by abnormal fractionated EGMs. Once identified, these areas were tagged on the electroanatomical map. After the baseline map was obtained, intravenous ajmaline was administered (10 mg/min) until a maximal target dose of 100 mg. Mapping of the BrS substrates was then repeated. We defined arrhythmogenic substrate sites as areas that harbored fractionated-EGMs, which were defined as ECGs that had: 1) low voltage (≤ 1 mV); 2) split EGMs or fractionated-EGMs with multiple potentials with ≥ 2 distinct components, with >20 ms isoelectric segments between peaks of individual components; and 3) wide duration (≥ 70 ms) of late potentials, with distinct potentials extending beyond the end of the QRS complex. The tissue area (cm^2) with abnormal fractionated EGMs was computed before and after ajmaline.

Four patients underwent the study during an open thoracotomy because they had pericardial adhesion precluding percutaneous access into the pericardium. After the anterior RVOT epicardium was exposed and clearly visualized, point-to-point mapping was used over these areas, in which numbers were assigned over a grid of the anterior RVOT and RV epicardium. A ThermoCool catheter was used for mapping and ablation. Mapping was performed at baseline and after ajmaline administration both during sinus rhythm and atrial pacing at the left atrial appendage. A biopsy also was performed at the sites where fractionated EGMs were recorded.

ECGI Mapping

ECGI methodology has been described previously⁴⁻⁶ and is presented in detail in the Supplemental Text 1. Activation mapping was performed during sinus rhythm at baseline and after ajmaline administration. The method of reconstruction of the epicardial activation pattern is also detailed in Supplemental Text and Supplemental Figure 1. We measured maximum STE and minimum voltage of unipolar ECG within the late activation zone before and after ajmaline.

Radiofrequency Ablation

Radiofrequency ablations were performed with power from 20-50 W, and the maximum temperature was set at 45°C. The primary end point during ablation was the elimination of the arrhythmogenic fractionated ECGs that were identified both during baseline and after ajmaline.

Clinical End Points and Follow-up

All patients were followed up at 1 month after the ablation session and every 3 months thereafter. Ajmaline provocative testing was performed after the 3-month follow-up. The long-

term end points were death and VF episode(s), as detected by ICD interrogation and presence of Brugada ECG pattern.

Data and Statistical Analysis

Paired student *t*-test was used to compare baseline and ajmaline conditions. Fisher exact test or Chi-square test was used for categorical data wherever appropriate. All data were analyzed with a statistical package, SAS version 9.2.

Results

Our 32 study patients were highly symptomatic with frequent ICD discharges due to VF (Table 1); 28 underwent mapping and ablation percutaneously and the remaining 4 via thoracotomy.

Effects of Pacing and Ajmaline on ECG Variables, ECG Duration, and Conduction

Fractionated EGMs were recorded in all patients at the anterior RVOT epicardium and in 12 of the 32 patients (37%) in both anterior and inferior RV epicardium. Ajmaline increased the substrate size from $13.8 \pm 6.2 \text{ cm}^2$ to $24.2 \pm 8.6 \text{ cm}^2$ ($p = 0.0012$).

In general, higher atrial pacing rate uniformly increased the EGMs duration but the effect was moderate in the majority of the patients and quite large in the 2 patients (Supplemental Figure 2) who had the longest baseline EGMs durations. Fractionated EGM duration increased at a higher atrial pacing rate: At 750 ms, the fractionated-EGMs were $112 \pm 48 \text{ ms}$ and increased to $143 \pm 66 \text{ ms}$ ($p = 0.003$), measured during the shortest cycle length pacing that produced one-to-one AV conduction. Figure 1 shows an example of the effect of pacing cycle length on the fractionated-EGM characteristics, comparing coronary sinus pacing of 600 and 450 ms at

baseline (Figure 1A) and between 600 ms pacing at baseline and after ajmaline (Figure 1B). The bipolar EGMs recorded from the distal (ABLd) and proximal (ABLp) pair electrodes of the ablation catheter at the RVOT epicardium show fractionated-EGM potentials beyond the QRS; at baseline, the duration of the fractionated EGMs recorded from ABLd increased from 181 during pacing at 600 to 280 ms during pacing at 450 ms. Even during these remarkable changes in the EGM fractionation, there was no Brugada ECG pattern appearance until ajmaline administration (50 mg) and pacing at 600 ms cycle length (Figure 1B) which shows a profound effect of ajmaline on conduction: The bipolar EGMs recorded at the same RVOT epicardial site show the drug caused a further marked increase in conduction delay and conduction block, as shown by prolonged fractionated EGMs beyond the T wave, resulting in a variable increase in EGM duration ranging from 230 to 320 ms. The loss of amplitude of the bipolar EGMs of the last three complexes recorded from both ABLd and ABLp pairs (vertical arrows) is compatible with local activation failure (a long recording of 600 ms pacing after ajmaline is shown in the supplemental Video 1a & 1b to authenticate that the loss of EGMs amplitude were due to loss of excitation and not due to the loss of mapping catheter's contact). Note that lead V2 shows alternation of the ST-segment amplitude in such a way that the higher amplitude of the ST-segment was related to excitation failure and absence of local activation. Loss of amplitude of fractionated EGMs upon ajmaline administration of high-rate pacing was observed in 11 of 15 patients (73%).

Table 2 summarizes the effect of ajmaline on the ECG variables: Ajmaline increased the QRS duration by 22% (95% confidence interval [CI]: 7.5-37.7%; $p < 0.0001$); PR interval 18% (95% CI: 12.5-24%; $p < 0.0001$); QTc interval 8% (95% CI: 3-12.6%; $p = 0.001$); and ST-segment in the right precordial leads by 74% (95% CI, 74-161%; $p < 0.0001$).

ECGI Substrate Mapping

Figure 2 shows an example of ECGI maps from one of our patients (panel A) and compares 4 ECGI variables in the late activation zone: activation time, STE, voltage, and area of late activation zone, at baseline and after ajmaline infusion during sinus rhythm in 20 patients. Panel A demonstrates that ajmaline increases the activation time, STE, and area of the late activation zone, while reducing the EGM voltage in one of the study patients. In aggregate (Figure 2, panel B), ajmaline delayed the activation time (33%; $p = 0.003$) and increased local unipolar STE (70%; $p = 0.002$), while significantly reducing the voltage (unipolar) in the late activation zone (33.5%; $p = 0.016$).

Fibrosis and Fractionated EGMs in Direct Epicardial Mapping

Figure 3 shows an example of how ajmaline unmasked the arrhythmogenic substrate areas on the underlying anterior RVOT epicardium in a patient who underwent epicardial mapping during a thoracotomy. Ajmaline (30 mg IV) caused changes in bipolar and unipolar EGMs of areas 3, 8, and 13 from relatively normal EGMs to markedly abnormal fractionated EGMs, coinciding with an appearance of STE in the unipolar EGMs in these areas. In particular, the unipolar EGMs after ajmaline infusion have a monophasic morphology (resembling an action potential), especially at panels B, E, and G. This is a sign of absence of local activation (similar to that recorded from a monophasic action potential catheter)⁷. This phenomenon is present at sites 3, 8, and 13. Biopsies at sites 8 and 13 and their histology demonstrate marked epicardial fibrosis (panel D).

All 4 patients, whose mapping and ablation were done under open thoracotomy, had localized epicardial and interstitial fibrosis, which is associated with abnormal fractionated EGMs. Ajmaline not only unmasks the arrhythmogenic areas that might have been otherwise

thought to be a normal area of RVOT epicardium because of a normal EGM at baseline, but the drug could also cause excitation failure and asynchronous conduction in the substrate areas, as shown in Figure 4.

Figure 4A shows lead avF, and local bipolar and unipolar EGMs recorded from the RVOT epicardium of another patient who underwent open thoracotomy. The bipolar EGMs recorded from the distal and proximal pair electrodes (ABLd and ABLp) and the unipolar EGM recorded from the distal electrode of the ablation catheter (ABLd uni) show prolonged fractionated EGMs at baseline. After ajmaline, the EGMs' duration drastically changed and became markedly delayed with multiple components and with the EGM duration of 350 and 305 ms at the ABLd and ABLp recording sites, respectively. The unipolar recording of the distal electrode of the 1st complex also showed multiple potentials, suggesting zig-zag conduction at the subepicardial tissue below the recording epicardial site. These late potentials were absent in the 2nd complex, indicating the conduction block at the subepicardial site; as a result, the ABLd uni of this complex also had a monophasic component (indicated in red).

Figure 4B shows the recording of another RVOT substrate site of the same patient. At this site, delayed conduction, asynchronous activation, and intermittent conduction blocks were demonstrated. The duration of fractionated EGMs at these sites was variably and markedly lengthened with intermittent conduction block causing a significant degree of dispersion of conduction between the distal and proximal pairs. Excitation failure was also seen between the distal and proximal pairs. Comparison with complexes 1 and 5 shows that these waves are distinct from the local T waves. When conduction blocks occurred in the distal pair of bipolar recording, monophasic components emerged in the unipolar EGMs. Biopsy at this site revealed thick epicardial fibrosis and fibrotic replacement in the sub-epicardium (Figure 4C).

Long-Term Outcomes

After one ablation procedure, type 1 Brugada ECG pattern disappeared in all but 2 patients who had Brugada ECG pattern after ajmaline. After a mean follow-up period of 50 ± 18 (median 48) months, 31 of the 32 patients had no VF recurrence; the remaining patient with VF recurrence had concomitant J-wave elevation in the inferior leads, hence a combined syndrome of BrS and the early repolarization pattern. The patient is expected to be scheduled for repeat ablation. The 2 patients who continued to have type 1 Brugada ECG pattern had no VF recurrence.

Discussion

Our study provides new insights into how ajmaline unmasks the Brugada ECG pattern: The drug, by reducing I_{Na} , markedly delays impulse conduction in these RVOT substrate sites that have underlying fibrosis, thereby increasing the areas of the late activation and in turn increasing STE over the right precordial ECG leads. This is associated with local STE and local loss of amplitude of the unipolar EGMs, as detected by ECGI. Furthermore, ajmaline unmasks the substrate by creating excitation failure, showing as the genesis of monophasic EGMs or as late monophasic components of unipolar EGMs in fibrotic tissue (Figure 3). In short, when I_{Na} is reduced, by rapid pacing or ajmaline administration, impulse conduction in the RVOT epicardial fibrotic substrate sites is severely compromised. This causes asynchronous conduction, conduction block, and/or excitation failure, leading to loss of local activation at these sites. These electrophysiologic derangements are the underlying mechanism of the STE in the right precordial leads and VF genesis in BrS.

Conduction Abnormalities After High Atrial Pacing Rate

The duration of fractionated EGMs was significantly further prolonged when atrial rate increased in all patients. The increased EGM duration after shortening of the pacing cycle length suggests a further increase in conduction abnormality, a well-known frequency-dependent response of conduction in the diseased tissue^{8,9}.

Unmasking the Brugada ECG by Ajmaline

Epicardial and interstitial fibrosis was found in all 4 patients who underwent open thoracotomy for mapping, surgical radiofrequency ablation, and subsequent study of the biopsies. The EGMs at the sites where fibrosis was present could be relatively normal, as shown in Figure 3; they only became markedly abnormal after ajmaline. In some areas, conduction block or asynchronous conduction occurred along with the appearance of the Brugada ECG pattern. Remarkably, monophasic unipolar EGMs were recorded after ajmaline administration as a sign of absence of activation, even though the tissue was intrinsically excitable. This is in line with the *in silico* and experimental observations of Hoogendijk et al.¹⁰ and that of Vigmond et al.¹¹, who show that monophasic-like local electrograms at the epicardial side of the RVOT could be recorded as a result of current-to-load mismatch owing to structural abnormalities.

Figure 5 displays the mechanisms causing monophasic EGMs during excitation failure. The figure duplicates the first two complexes from Figure 4. Complex 1 shows a local fractionated unipolar EGM with local ST-elevation in ABLd-uni with an appearance of a small monophasic complex. This is caused by myocardium under the electrode ABLd-uni that was not activated, leaving the membrane potentials at the resting potential. Since this myocardium is electrically coupled to the surrounding myocardium, it will become a current sink (intracellular)

when the surrounding myocardium depolarizes. This means the myocardium at electrode ABLd-uni will receive intracellular current that is transferred to the extracellular space where it can be recorded as a positive potential (monophasic action potential) with shape of the transmembrane potential of the surrounding myocardium. In complex 1, the amplitude of the local unipolar EGM (or monophasic complex) is small, but still looks like a V1 of type 1 Brugada pattern. In the complex 2, a larger part of the myocardium located at ABLd-uni is not activated during the first activation wave “a” but the myocardium under the proximal pair is activated late by activation wave “d”. The late activated myocardium at ABLp-uni will provide the intracellular current that flows to the myocardium at ABLd-uni and give rise to a monophasic complex in the extracellular space recorded at ABLd-uni.

Even though abnormal fractionated EGMs were present at the anterior RVOT in all our patients, many patients initially did not have a spontaneous type 1 Brugada ECG pattern. Thus, localized fractionation and late conduction at the RVOT alone may not be enough to cause the type 1 Brugada ECG pattern. The signature Brugada ECG pattern appeared only after ajmaline was administered in many of our patients and monophasic unipolar EGMs were recorded. This was associated with further prolongation of these abnormal epicardial EGMs and conduction block or excitation failure, as shown in Figure 1. Clearly, conduction block in various areas of the anterior RVOT epicardial substrate sites was instrumental in unmasking the type 1 Brugada ECG pattern. This is supported by the observation that small changes in activation contributed to subtle changes in the ECG ST-segment.

These findings support those of Hoogendijk and colleagues,¹⁰ as well as ten Sande et al.,¹² which suggest that, subepicardial structural abnormalities (in our study BrS patients, subtle fibrosis in the epicardium and sub-epicardium) are present in BrS patients and likely serve as the

barriers that create the tortuous path through which the propagating impulses have to go, and in turn create fractionated-EGMs and late potentials; these fibrotic tissues may also create a narrow isthmus for the depolarizing current to travel through and then reach the area of large expansion of the myocardium mass where “current-to-load mismatch” occurs, especially in the presence of reduced I_{Na} by ajmaline, causing excitation failure. The excitation failure can be intermittent or cycle length dependent, resulting in intermittent loss of local activation. The combined tissue discontinuity, excitation failure, and loss of local activation lead to the presence of STE in the right precordial leads because of the electronic current generated by activation of the proximal site through the isthmus.

This observation is therefore consistent with previous studies. In a study of an explanted heart of a BrS patient who had recalcitrant electrical storms necessitating heart transplantation surgery, Coronel et al. found abundant fibrous and adipose tissue in the RV associated with marked activation delay in the RV¹³. Our recent collaborative multicenter study unequivocally demonstrated epicardial and interstitial fibrosis and reduced gap junction expressions in the RVOT of sudden cardiac death victims with BrS family history and negative routine autopsy¹⁴. In the same study, we also found epicardial and interstitial fibrosis from the biopsies taken from BrS patients during open-heart ablation from RVOT epicardial sites; at these sites, abnormal, fragmented, and delayed conduction were also found¹⁴. Thus, the above observation incontrovertibly support that RV epicardium is the main substrate site where fractionated late ventricular electrograms are present in BrS patients as an expression of the structural abnormalities^{3, 14, 15}

Study Limitations:

Our study patients were highly selective of symptomatic patients and only 3% of our patients had SCN5A pathogenic variants, thus our study population may not be representative of general BrS population. Our GWAS study shows that SCN5A in Thai BrS population is only 7%¹⁶. However, we share the same findings as those of the Europeans' and Japanese's that BrS phenotype in our population is associated with polygenic variants including SCN5A, Hey2 and SCN10A¹⁶. Thus, we believe that our population is a not a unique subset.

The number of patients (n = 4) in this study who underwent biopsy of the RVOT substrate sites is relatively small. It is conceivable that not all BrS patients may have extensive fibrosis, as witnessed in our 4 study patients. However, we have so far studied 4 other patients who underwent open thoracotomy (not included in this study); they all had epicardial and subepicardial fibrosis. Thus, it is very likely that most BrS patients had subtle RV fibrosis as the primary underlying pathology and that our clinical observation of reduced I_{Na} is very likely applicable to BrS. However, since our study patients are highly symptomatic, the degrees of conduction abnormalities and fibrosis in asymptomatic patients may not be as severe as observed in our study patients. Indeed, it would be interesting to carry out studies to determine the relationship between the magnitude/severity of these abnormalities and the incidence and severity of VT/VF occurrences in BrS patients.

Conclusions:

Our study clearly shows that I_{Na} reduction with ajmaline and/or high rate pacing severely compromises impulse conduction in the BrS substrates and can uncover the fibrotic sites by producing fractionated EGMs, conduction block, or excitation failure that create milieu for

current-to-load mismatch phenomenon that leads to VF genesis and the signature Brugada ECG pattern. Ajmaline also is useful in guiding catheter ablations to eliminate all arrhythmogenic areas, as evidenced by a two-fold increase in the size of the target area for the ablation. Thus, using sodium channel blockers, ajmaline, or pilsicainide is an invaluable tool to guide catheter ablation of BrS substrates for better long-term outcomes^{3, 17, 18}.

Journal Pre-proof

References

1. Veerakul G, Nademanee K. Brugada syndrome: two decades of progress. *Circ J* 2012;76:2713-22.

2. Hoogendijk MG, Potse M, Linnenbank AC, et al. Mechanism of right precordial ST-segment elevation in structural heart disease: excitation failure by current-to-load mismatch. *Heart Rhythm* 2010;7:238-48.
3. Nademanee K, Veerakul G, Chandanamattha P, et al. Prevention of ventricular fibrillation episodes in Brugada syndrome by catheter ablation over the anterior right ventricular outflow tract epicardium. *Circulation* 2011;123:1270-9.
4. Ramanathan C, Ghanem RN, Jia P, Ryu K, Rudy Y. Noninvasive electrocardiographic imaging for cardiac electrophysiology and arrhythmia. *Nat Med* 2004;10:422-8.
5. Ramanathan C, Jia P, Ghanem R, Ryu K, Rudy Y. Activation and repolarization of the normal human heart under complete physiological conditions. *Proc Natl Acad Sci U S A* 2006;103:6309-14.
6. Nademanee K, Haïssaguerre M, Hocini M, et al. Mapping and ablation of ventricular fibrillation associated with early repolarization syndrome. *Circulation* 2019;140:1477-90.
7. Coronel R, de Bakker JM, Wins-Schopman FL, Linnenback AG, Belterman CN, Janse MJ. Monophasic action potentials and activation recovery intervals as measure of ventricular action potential duration. Experimental evidence to resolve some controversies. *Heart Rhythm* 2006; 3:1043-50.
8. Kawara T, Derksen R, de Groot JR, et al. Activation delay after premature stimulation in chronically diseased human myocardium relates to the architecture of interstitial fibrosis. *Circulation* 2001;104:3069-75.
9. Saumarez RC, Pytkowski M, Sterlinski M, et al. Paced ventricular electrogram fractionation predicts sudden cardiac death in hypertrophic cardiomyopathy. *Eur Heart J* 2008;29:1653-61.

10. Hoogendijk M, Opthof T, Postema PG, Wilde AA, de Bakker JJ, Coronel R. The Brugada ECG pattern: a marker of channelopathy, structural heart disease, or neither? Toward a unifying mechanism of the Brugada syndrome. *Circ Arrhythm Electrophysiol* 2010;3:283-90.
11. Vigmond EJ, Efimov IR, Rentschler SL, Coronel R, Boukens BJ. Fractionated electrograms with ST-segment elevation recorded from the human right ventricular outflow tract. *Heart Rhythm Case Reports* 2017;3:546-50.
12. ten Sande JN, Coronel R, Conrath CE, et al. ST-segment elevation and fractionated electrograms in Brugada syndrome patients arise from the same structurally abnormal subepicardial RVOT area but have a different mechanism. *Circ Arrhythm Electrophysiol* 2015;8:1382-92.
13. Coronel R, Casini S, Koopmann TT, et al. Right ventricular fibrosis and conduction delay in a patient with clinical signs of Brugada syndrome: a combined electrophysiological, genetic, histopathologic, and computational study. *Circulation* 2005;112:2769-77.
14. Nademanee K, Raju H, De Noronha S, et al. Fibrosis, connexin 43, and conduction abnormalities in the Brugada syndrome. *J Am Coll Cardiol* 2015;66:1976-86.
15. Behr ER, Ben-Haim Y, Ackerman MJ, Krahn AD, Wilde AA. Brugada syndrome and reduced right ventricular outflow tract conduction reserve: a final common pathway? *Eur Heart J* 2021;42:1073-81.
16. Makarawate P, Glinge C, Khongphatthanayothin A, et al. Common and rare susceptibility variants predisposing to Brugada Syndrome in Thailand. *Heart Rhythm* 2020;17:2145-2153

17. Pappone C, Brugada J, Vicedomini G, et al. Electrical substrate elimination in 135 consecutive patients with Brugada syndrome. *Circ Arrhythm Electrophysiol* 2017;10:e005053.
18. Nademanee K, Hocini M, Haïssaguerre M. Epicardial substrate ablation for Brugada syndrome. *Heart Rhythm* 2017;14:457-61.

Journal Pre-proof

Figure Legends

Figure 1. The effects of pacing and ajmaline on the BrS substrate sites are illustrated (see text for details). Figure 1A shows the effect of shortening of the pacing cycle length from 600 to

450 ms (coronary sinus pacing) on the electrogram duration at the RVOT epicardial substrate site. Figure 1B shows a conduction block at the same site as Figure 1A, after ajmaline during pacing at 600 ms. V2 IC3 = Lead V2 at the 3rd intercostal space. ABLd = ablation distal pair electrodes; ABLp = ablation proximal pair electrodes; RVAp = right ventricular apex proximal pair electrodes; Stim = stimulation artefact.

Figure 2. Panel A shows an example of ECGI maps from one of the study patients, displaying activation time, ST elevation (STE), voltage, and areas of the late-activated area before and after ajmaline during sinus rhythm. Panel B summarizes results from the analyses of all patients within the late activation zone.

Figure 3. Computed tomography scan of the heart (center) from 1 of the 4 BrS patients undergoing open thoracotomy mapping and ablation showing RV anatomical grid. ECG lead II and a distal bipolar (0.4 mV/cm voltage scale at the filter 30 Hz-300 Hz) and unipolar electrogram (5 mV/cm voltage scale at the filter 0.05 Hz-300 Hz) are displayed in insets of the surrounding panels. Clockwise from the right are panels A and B, which display electrograms from site 8 at baseline and after ajmaline, respectively; panel C shows electrograms recorded from site 9 after ajmaline; panel D is histology of the biopsy specimen (Masson's trichrome stain) from site 8 showing epicardial fibrosis; panels E and F and panels G and H display electrograms recorded from sites 13 and 3 after ajmaline and at baseline, respectively (see text for details).

Figure 4. Figures 4A and 4B show ajmaline produced delayed conduction, asynchronous activation, and conduction block causing monophasic appearance of the unipolar recording at that site (pink shade on the ABLd-uni). Figure 4C shows hematoxylin and eosin (H&E) stain of

the biopsy from this recording site and shows marked epicardial fibrosis and early fibrotic replacement of the myocardial at this site (orange arrow).

Figure 5. A schema to explain how ajmaline delayed conduction and caused excitation failure of the first two impulses in Figure 4B, producing monophasic unipolar ECG pattern (see text for details).

Journal Pre-proof

Table 1. Patient Clinical Characteristics

Number of patients	32
Age	40 ± 12 (median 37) years
Gender	All males

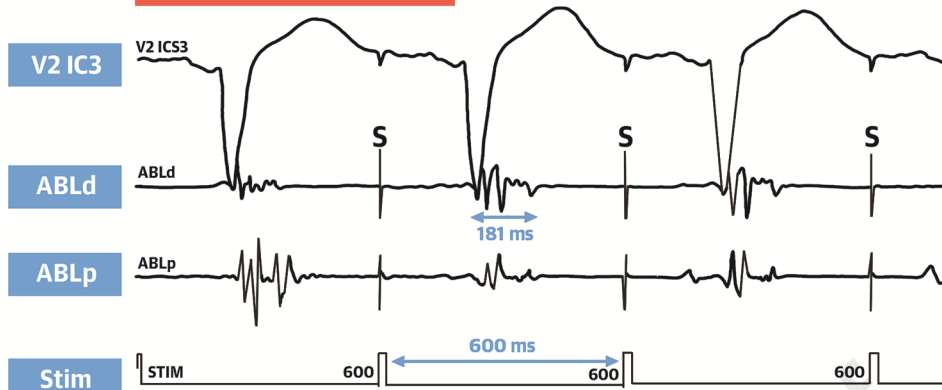
Symptoms	Aborted cardiac arrests/VF = 30 (94%) Syncope = 2 (6%)
Family history	10 (31%)
Spontaneous Brugada ECG pattern	28 (88%)
Distribution of patients according to total number of VF episodes on ICD	No episode = 4 (12%) 1-4 episodes = 6 (19%) 5-9 episodes = 2 (6%) 10-20 episodes = 5 (16%) >20 episodes = 15 (47%)
SCN5A mutation (only 29 had completed genetic study)	1 of 29 (3%)
Sustained VT/VF by PES at baseline	Positive 31 (97%); Negative 1 (3%)

Table 2. Effect of Ajmaline on ECG parameters and RVOT Substrate Size

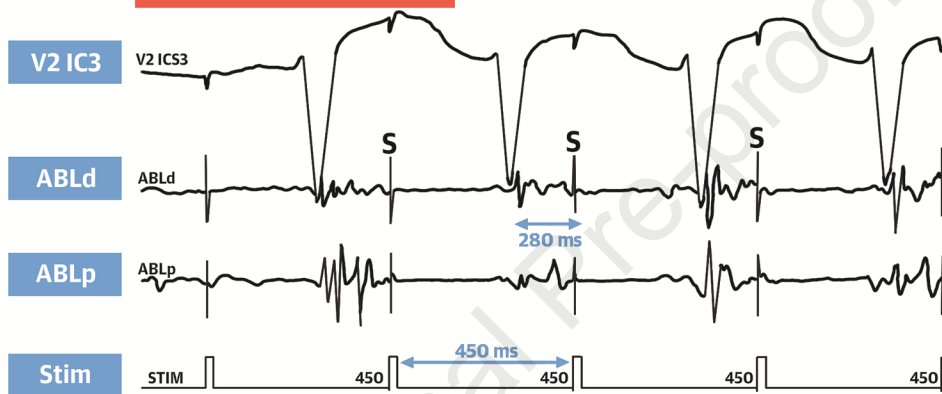
Variables	Baseline (Mean ± Std)	Ajmaline (Mean ± Std)	% Difference from baseline (95% CI)	P Value
CCL (msec)	923 ± 180	884 ± 171	-4.2% (-3% to 11.5%)	0.241
PR (msec)	176 ± 31	208 ± 38	18% (12.5% to 24%)	<0.0001
QRS (msec)	106 ± 22	130 ± 44	22.6% (8% to 38%)	0.005
QTc (msec)	415 ± 44	449 ± 49	8% (3% to 12.6%)	0.001
ST-seg (mV)	0.31 ± 0.19	0.54 ± 0.26	74% (45% to 161%)	<0.0001
RVOT-subst	13.7 ± 5.9	23.9 ± 8.2	74% (58% to 91%)	<0.0001

1A

Baseline Pacing (600 ms)

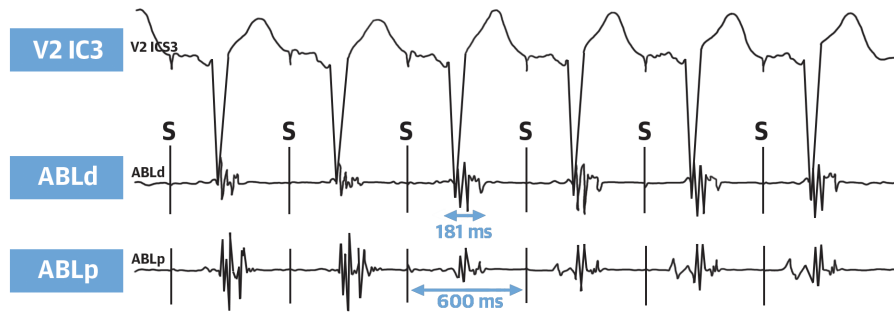


Baseline Pacing (450 ms)

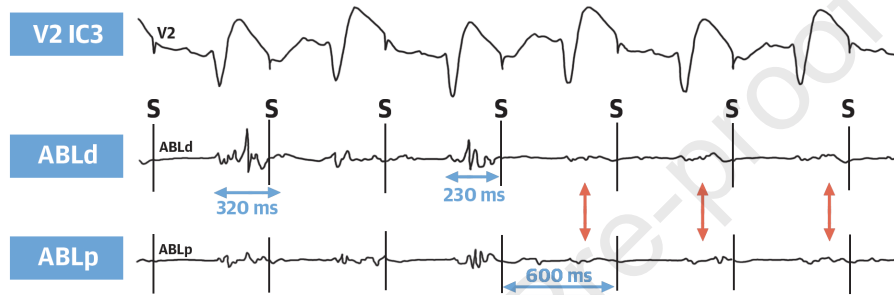


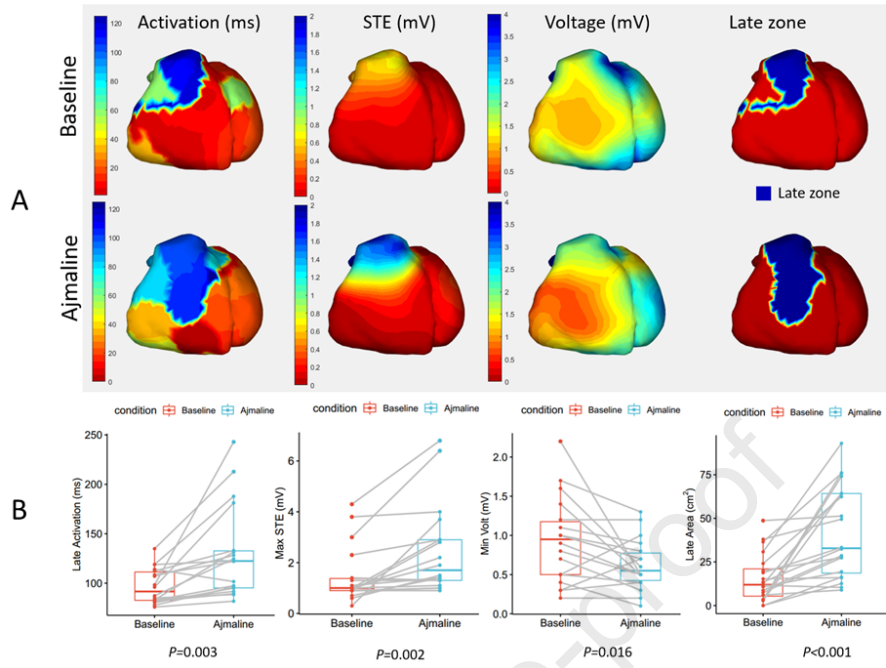
1B

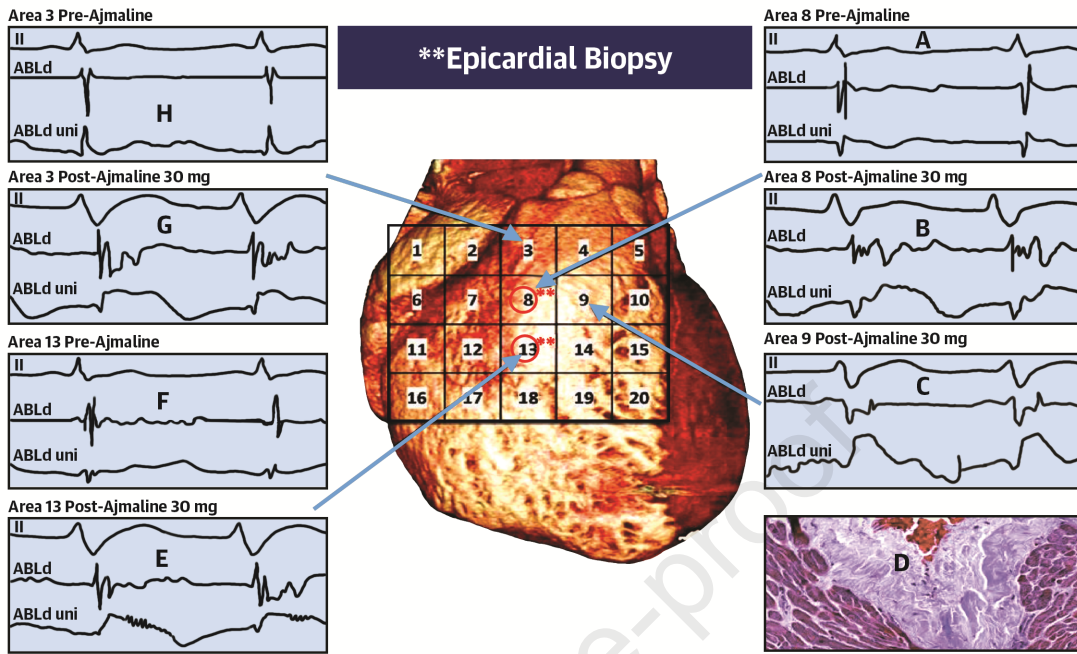
Baseline Pacing (600 ms)

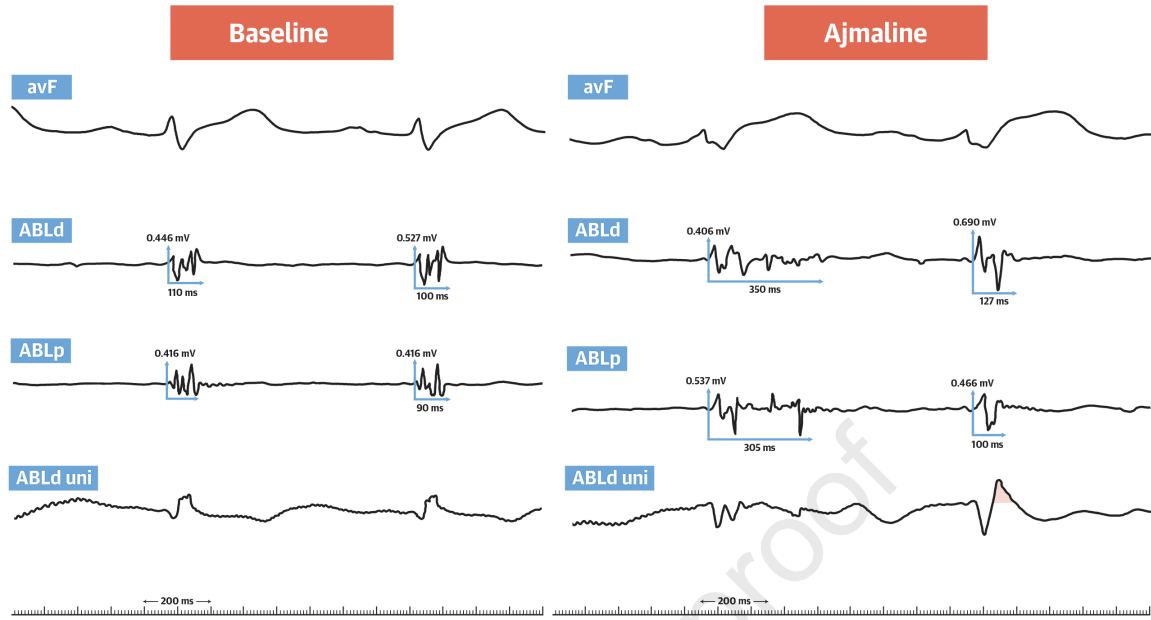


Ajmaline Pacing (600 ms)

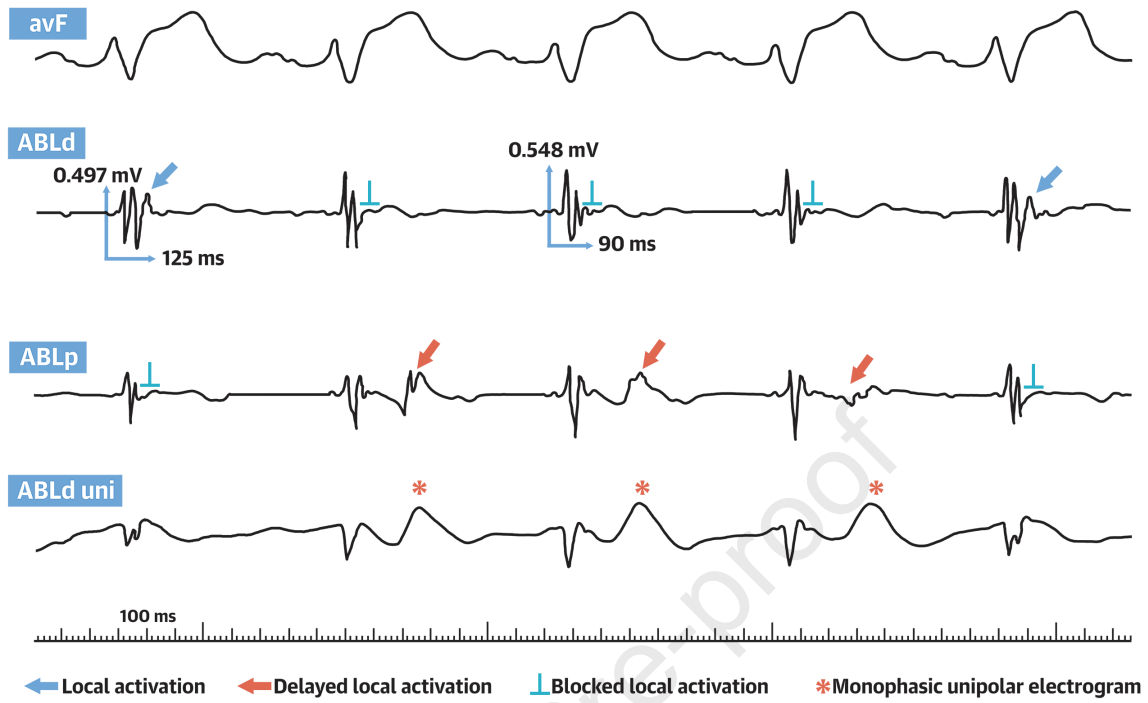


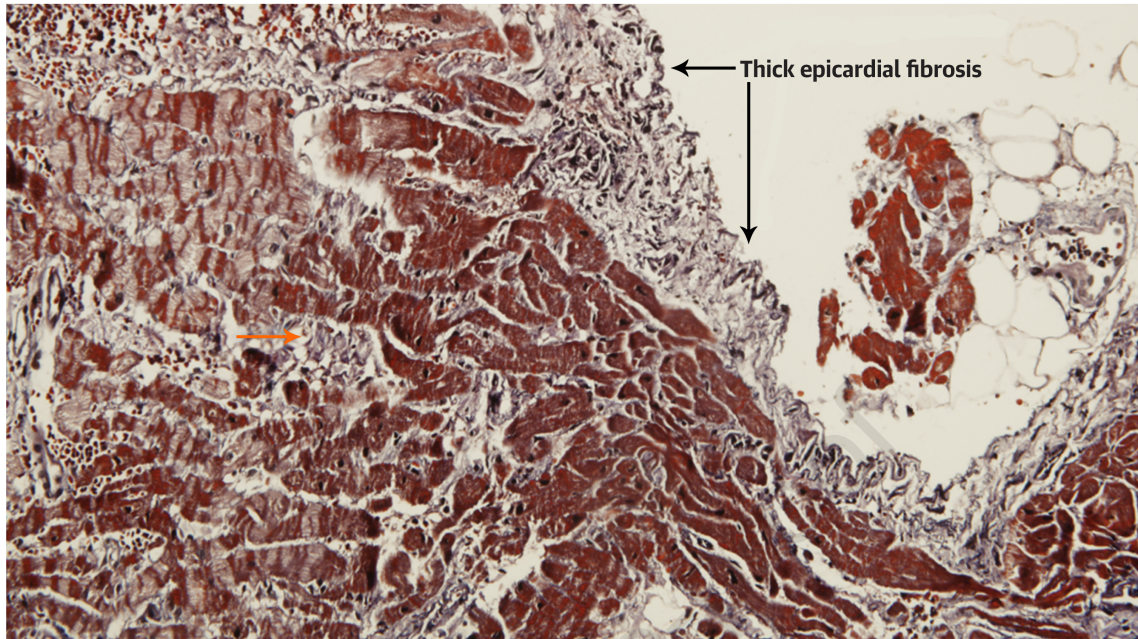






Journal Pre-proof





Journal Pre

